



This open access document is published as a preprint in the Beilstein Archives with doi: 10.3762/bxiv.2019.55.v1 and is considered to be an early communication for feedback before peer review. Before citing this document, please check if a final, peer-reviewed version has been published in the Beilstein Journal of Nanotechnology.

This document is not formatted, has not undergone copyediting or typesetting, and may contain errors, unsubstantiated scientific claims or preliminary data.

**Preprint Title** On tuning architectonics of nanoscaled assemblies of Zn-Ga-Al  
-based oxides obtained from layered double hydroxides precursors

**Authors** Corina E. Ignat, Gabriela Carja, Laura E. Romila and Doina Lutic

**Article Type** Full Research Paper

**ORCID® iDs** Gabriela Carja - <https://orcid.org/0000-0002-5568-4097>; Laura E. Romila - <https://orcid.org/0000-0002-6451-4903>; Doina Lutic - <https://orcid.org/0000-0002-3959-0891>

# On tuning architectonics of nanoscaled assemblies of Zn-Ga-Al - based oxides obtained from layered double hydroxides precursors

Corina Eugenia Ignat<sup>1</sup>, Gabriela Carja\*<sup>1</sup>, Laura Ecaterina Romila<sup>3</sup>, Doina Lutic\*<sup>2</sup>

<sup>1</sup>*Faculty of Chemical Engineering and Environmental Protection, Technical University of Iasi, 71 D.*

*Mangeron, Iasi, Romania, e-mails: : [ignat.corina0702@gmail.com](mailto:ignat.corina0702@gmail.com), [carja@uaic.ro](mailto:carja@uaic.ro)*

<sup>2</sup>*Faculty of Chemistry, Al. I. Cuza University of Iasi, 11 Bd. Carol I, 700506 Iasi, Romania, e-mail:*

*[doilub@yahoo.com](mailto:doilub@yahoo.com)*

<sup>3</sup>*Faculty of Dentistry, Apollonia University of Iasi, 2 Muzicii Street, 700399, Iasi, Romania, e-mail:*

*[laura.dartu@gmail.com](mailto:laura.dartu@gmail.com)*

\* Corresponding author e-mail: [carja@uaic.ro](mailto:carja@uaic.ro); [doilub@yahoo.com](mailto:doilub@yahoo.com)

## Abstract

Nanoscaled self-assemblies with engineered architectonics are important for obtaining innovative materials for different front-line applications. We investigated here the morphology features at the nanoscale of the assemblies of the mixed oxides obtained through the thermal transformation of  $\text{Zn}^{2+}\text{Me}^{3+}$  (Me=Al/Ga) layered double hydroxides (LDHs), as their “as-synthesized” form or after they were reconstructed in the aqueous solution of  $\text{Ga}_2(\text{SO}_4)_3$ . The characteristics of ZnMe LDHs and the derived assemblies of mixed oxides were assessed by X-ray diffraction (XRD), X-ray photoelectron spectroscopy (XPS), scanning electron microscopy (SEM), transmission electron microscopy (TEM/EDX),  $\text{N}_2$  adsorption at  $-196^\circ\text{C}$  and thermal analyses (TG/DTG/DSC). The results revealed the formation of nanoscaled assemblies of  $\text{ZnO}/\text{ZnAl}_2\text{O}_4/\text{ZnGa}_2\text{O}_4$  and  $\text{ZnO}/\text{Ga}_2\text{O}_3/\text{ZnGa}_2\text{O}_4$  derived from ZnMe (Me=Al/Ga) as

precursors. Results point out that both the composition of the LDHs and the calcination temperatures can be used as parameters for tuning the nanomorphology features of the evolved mixed oxides.

**Keywords:** mixed oxides, layered double hydroxides, nanoscaled assemblies

## 1. Introduction

Layered double hydroxides (LDHs) are anionic clays, containing divalent ( $\text{Me}^{\text{II}}$ ) and trivalent ( $\text{Me}^{\text{III}}$ ) cations, generally described by the formula:  $[\text{Me}^{\text{II}}_{1-x}\text{Me}^{\text{III}}_x(\text{OH})_2]^{x+} \cdot \text{A}^{n-}_{x/n} \cdot m\text{H}_2\text{O}$ . The cations are included in octahedral units and are surrounded by six  $\text{HO}^-$  groups. The octahedral units of the layered layers are connected to each other through  $\text{HO}^-$  groups belonging to the neighboring units, arranged in hexagonal packing, similar to that of brucite structure. LDHs have a 2-D layered crystal structure with wide variations depending upon the nature of cations and  $\text{Me}(\text{II})/\text{Me}(\text{III})$  molar ratios, as well as  $\text{A}^{n-}$  interlayer anions [1,2]. Further, the LDHs structure is stabilized by including a high number of water molecules in the interlayer space, through numerous hydrogen bonds established with both cationic sites from the brucite-type layer and the anions from the interlayers. Significant progress has been made in the synthesis of LDH as tailored heterobimetallic systems allowing specific conductive responses [1-3]. Furthermore, LDHs are easily synthesized by cost-effective experimental procedures [4, 5]. A unique behavior of the LDHs is so-called structural “memory effect”. Such that, the LDHs calcination at moderate temperatures within the range 400-600°C, might destroy the 2-D layered structure giving rise to assemblies of mixed oxides [6,7]. When these oxides are introduced in aqueous solutions containing anions, the layered structure of LDH is able to recover the original layered structure. [8-12]. The calcination temperature values have an important role during the transformation of the LDHs in the assemblies of mixed oxides and the reconstruction of the 2D network by the memory effect [10-12]. For the temperature values higher than 650°C, the transformations of the LDH into the mixed are irreversible, giving rise to stable nanoscaled assemblies of the mixed oxides

[7,11]. Scarce information exists in the literature regarding the nanoscaled morphology of the assemblies of the mixed oxides derived from LDHs and tuning the architectonics of the self-assemblies of the mixed oxides is still a challenge for growing them as innovative heterostructures.

In the present work we present for the first time Zn-Ga-Al -based oxides as nanoscaled assemblies obtained through the thermal transformation of  $Zn^{2+}Me^{3+}$  (Me = Al/Ga) layered double hydroxides (LDHs) by using either the LDHs in “as-synthesized” form or after the LDHs was reconstructed in the aqueous solution of  $Ga_2(SO_4)_3$ . Furthermore, the properties of these complex mixed oxides and their morphology features were studied as a function of the LDHs compositions and the LDHs calcination temperature.

## 2. Experimental

### Synthesis of the LDH-like materials

The LDHs precursors, denoted as ZnGa and ZnAl, were prepared by the co-precipitation method. In a typical synthesis procedure, mixed solutions of  $Zn(NO_3)_2 \cdot 6H_2O/Ga(NO_3)_3 \cdot 18H_2O$  and  $Zn(NO_3)_2 \cdot 6H_2O/Al(NO_3)_3 \cdot 9H_2O$ , respectively, with  $Zn^{2+}/Me^{3+}$  ratios of 3 (1M overall concentration of cations) were slowly poured together with a  $Na_2CO_3/NaOH$  solution in a beaker, under vigorous stirring. The pH of the precipitation medium was kept at a constant value of 8.5 by controlling the metallic salts and carbonate/hydroxide solutions flows at proper levels. The precipitate slurry was aged for 24 h at room temperature under slow stirring, then separated by filtration, washed three times with distilled water and dried at 80°C overnight. The samples calcined at 550°C for 8 hours (denoted ZnGa\_550 and ZnAl\_550) were subsequently introduced in an aqueous solution of  $Ga_2(SO_4)_3 \cdot 18 H_2O$  (0.1M) (99.9%, Sigma Aldrich) for 7 h, at room temperature, to allow the reconstruction of the original layered structure. The samples were denoted as Ga/ZnAl and Ga/ZnGa, respectively. Afterwards, the “as synthesized” and the reconstructed LDHs were calcined in air at 600, 750 and 925°C at 10°/min, for 5 hours. The samples were labeled as Ga/ZnAl\_t and Ga/ZnGa\_t, where t is the calcination temperature value (°C).

## Characterization techniques

The structural characteristics were analyzed by powder X-ray diffraction (XRD) on a Shimadzu XRD 6100 diffractometer with monochromatic light ( $\lambda=0.1541$  nm), operating at 40 kV and 30 mA,  $2\theta$  range 5-80°. The LDHs showed rhombohedral symmetry and the structural parameters were calculated using the relations:  $a = 2 d_{[110]}$  and  $c = 3 d_{[003]}$ , where the indexes indicate the orientations of these two characteristic planes. The morphology features of the samples were investigated using a transmission electron microscopy (TEM) Hitachi H900, operating at an accelerating voltage of 200 kV, coupled with energy dispersive X-ray (EDX) spectrometer and a scanning electron microscope (SEM) (Philips, XL30 FEG). The X-ray photoelectron spectroscopy (XPS) spectra were recorded on a Perkin-Elmer 5500-MT spectrometer, equipped with Mg K $\alpha$  radiation (1253.6 eV), operating at 15 kV and 20 mA; the binding energies (BE) were corrected using the C1s peak to 284.8 eV as reference. Thermal analyses of powdered sample up to 900°C were carried out at a heating rate of 10°C/min in nitrogen gas flow, using on a Perkin Elmer equipment consisting of a TG/DTG/DTA Diamond thermo-balance. Nitrogen adsorption–desorption isotherms were obtained at –196 °C using a Coulter SA 3100 automated gas adsorption system. The samples were outgassed under vacuum at 110 °C overnight in order to remove the interlayer water, before the measurements. Specific surface area was calculated according to the BET method on the basis of the adsorption data.

## 2. Results and discussions

The structural features of the studied materials are described by the XRD results. Fig. 1 shows that the XRD pattern of the “as synthesized” ZnAl and ZnGa displays a LDH single phase without any impurity, with a series of sharp, symmetric and basal reflections, corresponding to [003] and [006] planes and broad, less intense, non-basal reflections assigned to the [012], [015] and [018] planes. The reflections corresponding to [110] and [113] are clearly distinguished at  $2\theta$  around 60 degrees, pointing out a well-ordered layered clay matrix. The slight differences due to the different ionic volumes of Al and Ga changed the values of the maxima of the diffraction angles (Table 1).

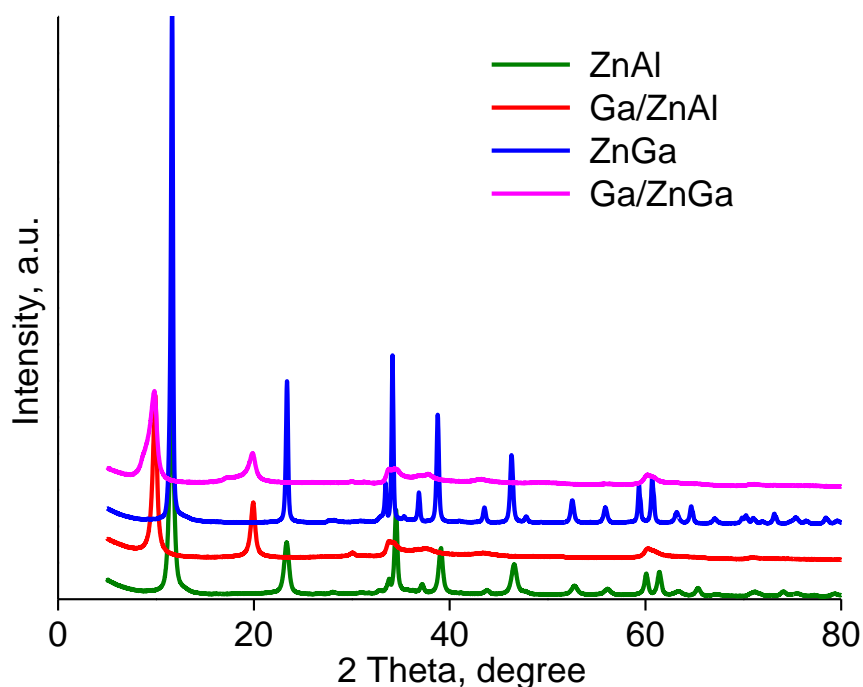


**Figure 1.** XRD patterns of the as-synthesized and the reconstructed LDH-like precursors.

After calcination at 550°C, the LDH structure collapsed and the characteristic allure of XRD of mixed oxides were obtained (not shown). The presence of the mixed oxides after the reconstruction in the  $\text{Ga}_2(\text{SO}_4)_3$  solution was demonstrated by the main characteristic planes ([003], [006], [110] and [113]) in the XRD pattern, confirming the success of the reconstruction process. The positions of the [003] and [110] planes were used to calculate the structural parameters of the samples (Table 1).

**Table 1:** XRD data and the calculated structural parameters for the as-synthesized and reconstructed samples

	ZnAl	ZnGa	Ga/ZnAl	Ga/ZnGa
$2\theta$ [003], °	11.61	11.64	9.89	9.79
$2\theta$ [006], °	23.34	23.39	20.00	19.96
$2\theta$ [101], °	33.82	33.47	33.86	33.80
$2\theta$ [009], °	34.53	34.17	36.91	38.8

$2\theta$ [110], °	60.55	59.35	60.55	60.19
$2\theta$ [113], °	61.44	60.69	61.44	60.70
$d$ [003], Å	7.61	7.59	8.94	9.03
$d$ [110], Å	1.53	1.56	1.53	1.54
$a$ , Å	3.06	3.11	3.06	3.07
$c$ , Å	22.83	22.77	26.82	27.09

It is important to underline that the XRD parameters changed after the reconstruction. Gallium phases were not found, indicating that, if present, gallium nanoparticles are too small to be detected by XRD. The values of the “ $c$ ” parameter increased, pointing out that the sulfate ions are present in the interlayer space and determined its expansion. As expected, the values of parameter “ $a$ ” is almost identical for all the samples, indicating that the reconstruction did not modify the distance between the cations of the brucite-like layers. For the reconstructed LDHs, the XRD peaks are wider, lower as intensity and not so well defined, indicating the partial loss in crystallinity and the decrease of the particle size.

For higher values of the calcination temperatures equal to 750°C and 925°C, the structural features are completely transformed, revealing the formation of the assemblies of the mixed oxides. For the series derived from ZnAl LDH precursor the XRD patterns are displayed in Figure 2.

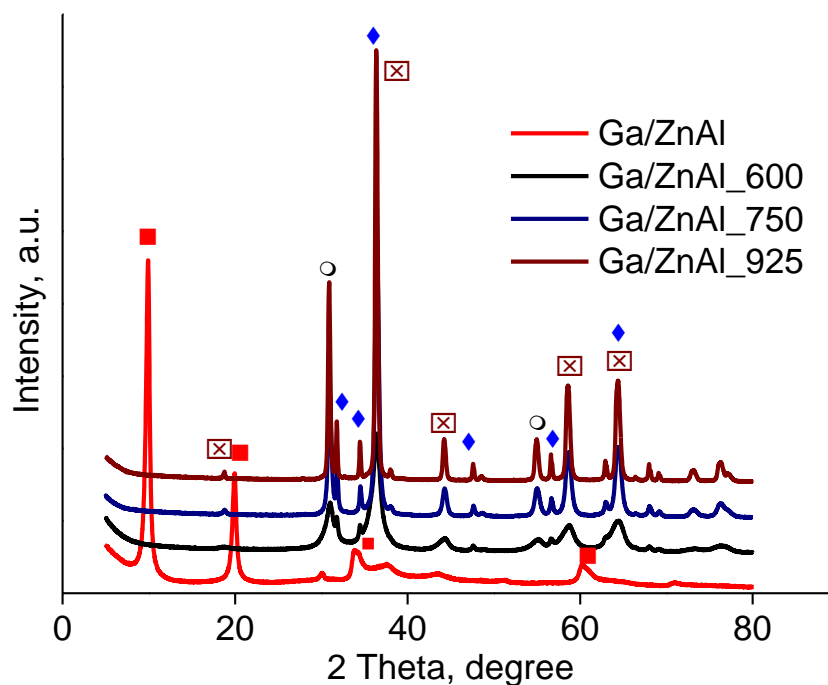


**Figure 2.** XRD patterns of the Ga/ZnAl and the mixed oxides obtained by calcination.

(■-LDH phase, ◆- ZnO, ○-ZnAl<sub>2</sub>O<sub>4</sub>, ☒- ZnGa<sub>2</sub>O<sub>4</sub>)

Ga/ZnAl showed the same trend: when the calcination temperatures increased, the extent of crystallization accentuated for higher temperature values. The peaks from the diffraction pattern clearly described the self-assembly of the mixed ZnO/ZnAl<sub>2</sub>O<sub>4</sub>/ZnGa<sub>2</sub>O<sub>4</sub> phases, as is detailed in Table 2. As the temperature increased, the peaks become higher, sharper and narrower, indicating that ZnO/ZnAl<sub>2</sub>O<sub>4</sub>/ZnGa<sub>2</sub>O<sub>4</sub> improved their crystallinity.

**Table 2:** The XRD parameters for the assemblies of the mixed oxides obtained by the thermal transformation of Ga/ZnAl and Ga/ZnGa LDHs.

Oxide phase	Maxima diffraction angles, 2theta (degrees) and planes indexes					
$\gamma$ -Al <sub>2</sub> O <sub>3</sub>	26	35	37	43	52.5	57
	[012]	[104]	[110]	[113]	[024]	[116]

ZnO	32 34.5 36.5 47.6 56.9 63.1 68.1 69.3 [100] [002] [101] [102] [110] [103] [112] [201]
ZnAl <sub>2</sub> O <sub>4</sub>	30 35 55 60 66 [220] [311] [422] [511] [440]
ZnGa <sub>2</sub> O <sub>4</sub>	19 31 35.5 38 43 55 58 63 [111] [220] [311] [222] [400] [422] [511] [440]
GaO(OH)	18 21.5 26 33.5 35 37.5 41 42 52 54 60 [020] [110] [120] [130] [021] [111] [121] [140] [211] [221] [151]
$\alpha$ -Ga <sub>2</sub> O <sub>3</sub>	24.8 33 36 41.5 50 55 63 65 [012] [104] [110] [113] [024] [116] [214] [300]
$\beta$ -Ga <sub>2</sub> O <sub>3</sub>	18 30 31.5 35 38.5 43 46 48 57.5 61 62.5 65 [20-1] [400] [002] [111] [311] [112] [600] [511] [313] [020] [-710] [221]

For the Ga/ZnGa the XRD patterns are displayed in Figure 3.

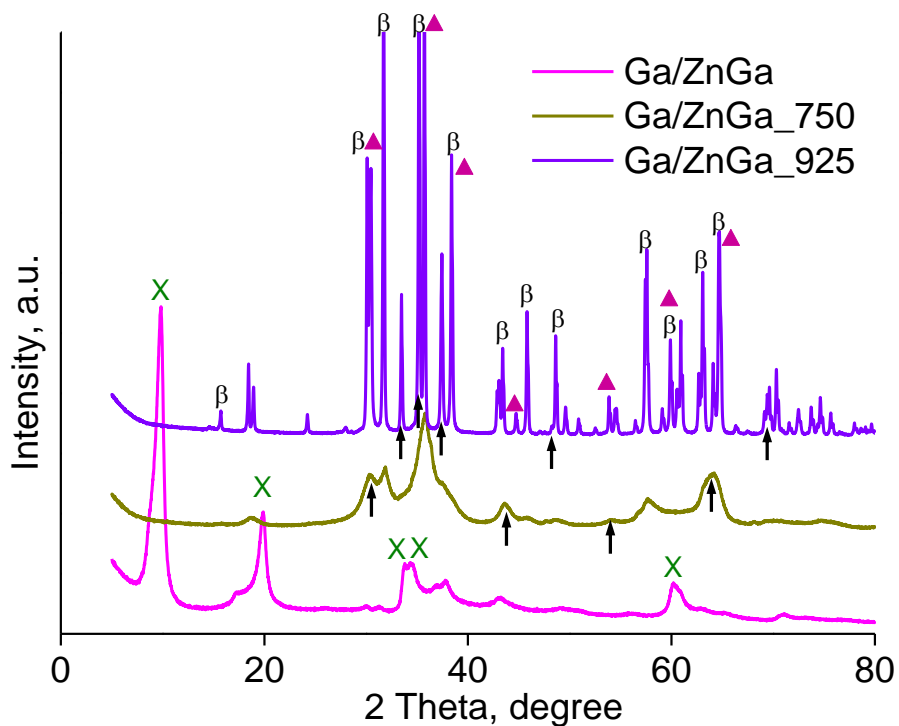


**Figure 3.** XRD patterns of Ga/ZnGa and the mixed oxides obtained by calcination.

( $\beta$  – beta  $\text{Ga}_2\text{O}_3$ ,  $\blacktriangle$   $\text{ZnGa}_2\text{O}_4$ ,  $\uparrow$   $\text{ZnO}$ ,  $\times$  - LDH).

Hence, after the calcination at  $750^\circ\text{C}$ , Ga/ZnGa display a low crystallinity mixed oxide, in which the reflection of  $\text{ZnO}$  and  $\text{ZnGa}_2\text{O}_4$  are clearly identified. After calcination at  $925^\circ\text{C}$ , the XRD analysis clearly show the formation of well-crystallized  $\beta$ - $\text{Ga}_2\text{O}_3$ , while the characteristic reflections of  $\text{ZnGa}_2\text{O}_4$  is also identified. This result is in agreement with previous reported data from the literature [13-22]. Therefore, the controlled thermal treatment of Ga/ZnGa gave rise to a complex assembly of the mixed oxides described as  $\text{ZnO}/\text{Ga}_2\text{O}_3/\text{ZnGa}_2\text{O}_4$ .

To get more information about the structural transformations, thermal analysis was performed from room temperature up to  $900^\circ\text{C}$ ; the TG and DTG curves are shown in Figure 4 and the mass loss and characteristic temperature values are shown in Table 3.

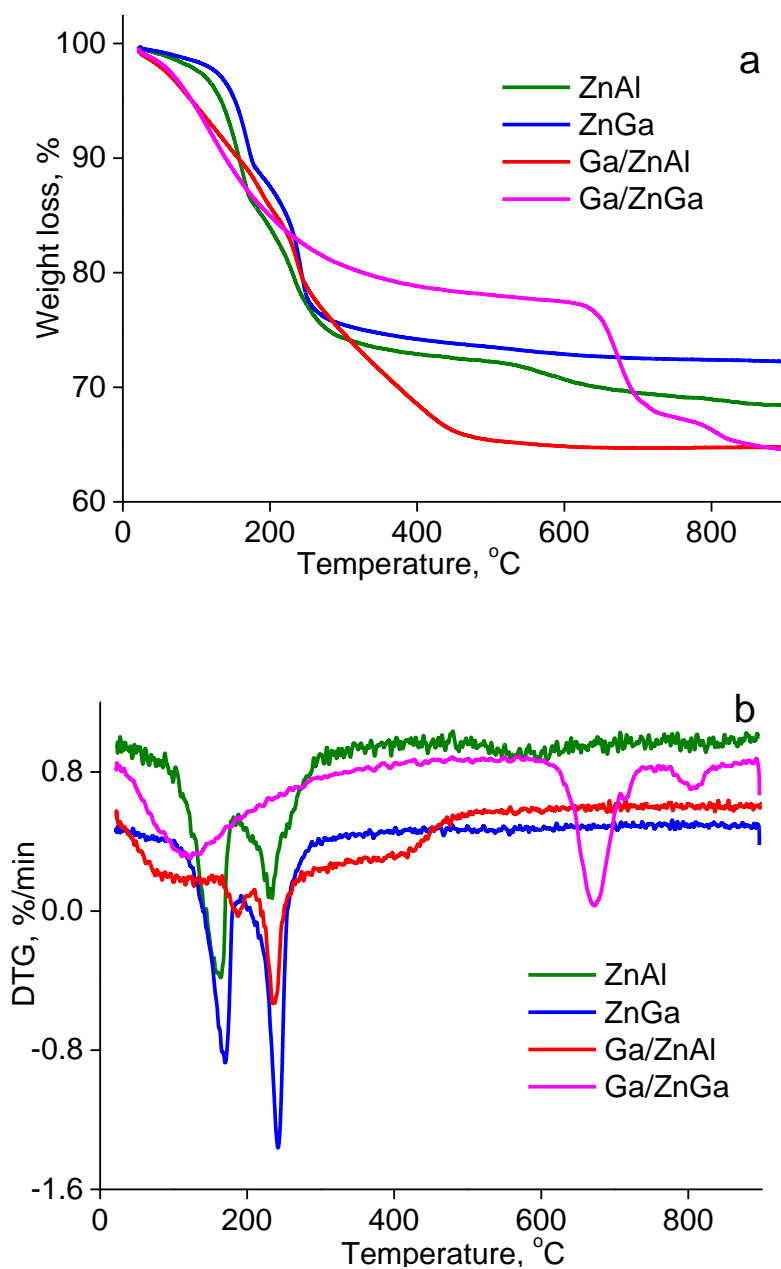


**Figure 4.** TG (a) and DTG (b) curves for the “as-synthesized” and the reconstructed LDHs.

The decomposition temperatures are slightly higher for Ga-containing LDH and the two weight loss stages were due to the water elimination from the interlayer and to the decomposition of the  $\text{HO}^-$  and, most probably,  $\text{NO}_3^-$  anions, respectively. In the case of the initial ZnAl and ZnGa LDHs, the mass loss reported in terms of moles of was almost similar for both samples.

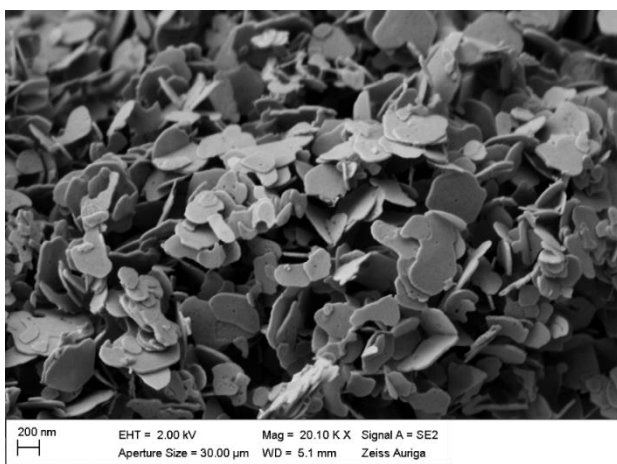
**Table 3:** Thermal analysis results

Sample	Characteristic temperatures		% mass loss
ZnAl	163	233	31.55
ZnGa	170	242	28.75
Ga/ZnAl	187	237	35.22
Ga/ZnGa	123	672	35.44

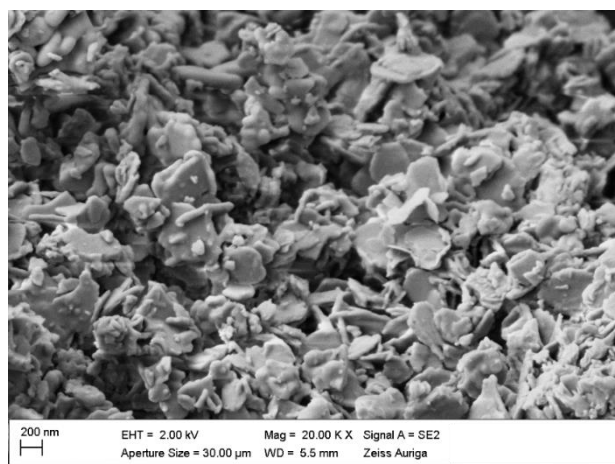
Assuming the chemical composition of  $Zn_3Al(OH)_8NO_3$  for ZnAl and  $Zn_3Ga(OH)_8NO_3$  for ZnGa, the "molar masses" of these species are, 421.2 respectively 463.9. After the thermal degradation, the mass loss ratios for the both samples are 288.1 and 330.5, as shown in Table 4. Ideally, the mixed oxides resulted by calcination have the formulae  $Zn_3AlO_{4.5}$  (mass 295.2) and  $Zn_3GaO_{4.5}$  (mass 337.9). The ratio between the calculated and experimental mass changes for both samples is 1.02. For the reconstructed samples, Ga/ZnAl and Ga/ZnGa, the weight loss has almost similar values. However, in the case of Ga/ZnGa sample, the decomposition temperature is much higher than for Ga/ZnAl. It is a prove that sulfate anions entered in the interlayer as compensation anions in a higher extent during the reconstruction of the calcined ZnGa. This statement is also supported by the bigger value of the  $c$  parameter of the cell (Table 1) and by the presence of high amounts of sulfur in the Ga/ZnGa reconstructed sample (Table 3). The temperature of the second decomposition step of Ga/ZnAl sample is in turn similar to the initial samples, suggesting that in this case, the reconstruction was performed including rather by  $HO^-$  ions in the interlayer, not  $SO_4^{2-}$  ions.

The nanoscale morphology of the starting LDHs and the assemblies of the mixed oxides was analyzed by SEM and TEM microscopy. SEM images of some representative samples are shown in Figures 5 and 6.

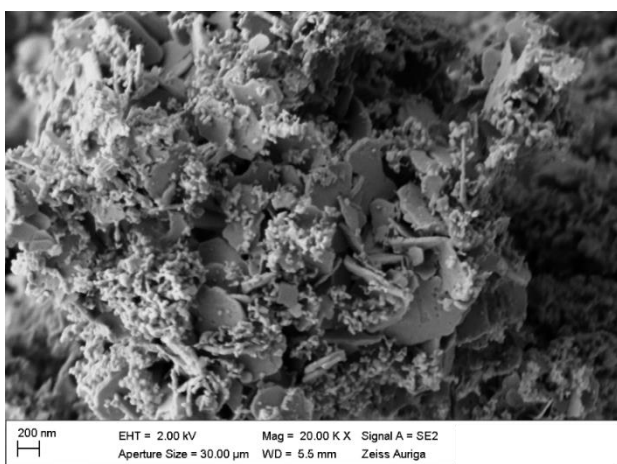
ZnGa



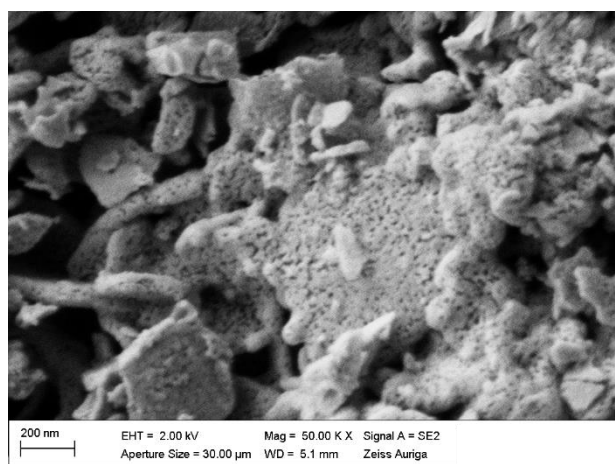
Ga/ZnGa



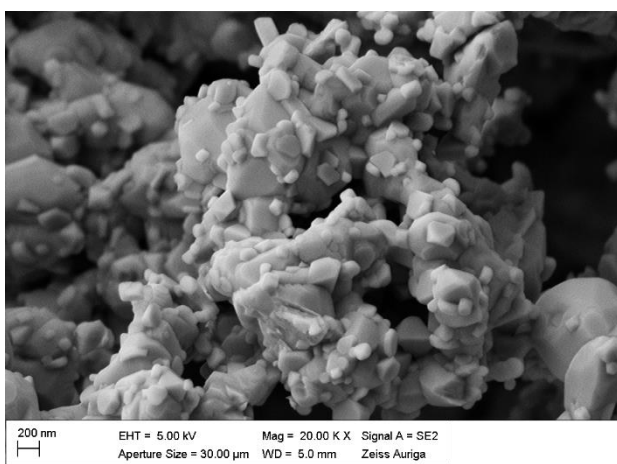
ZnGa\_750



Ga/ZnGa 750



ZnGa\_925



Ga/ZnGa 925

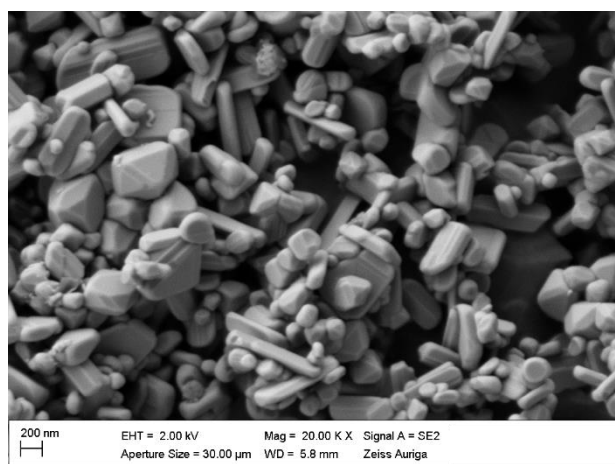
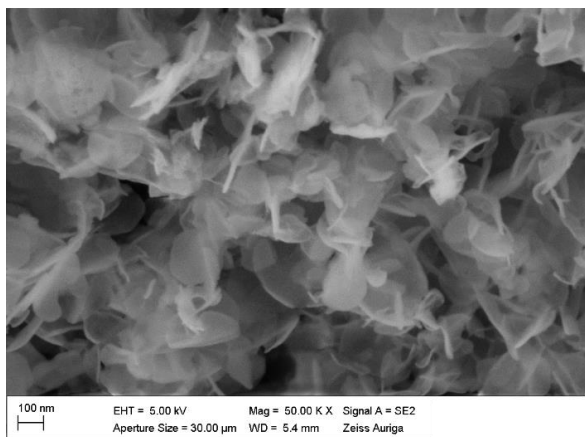
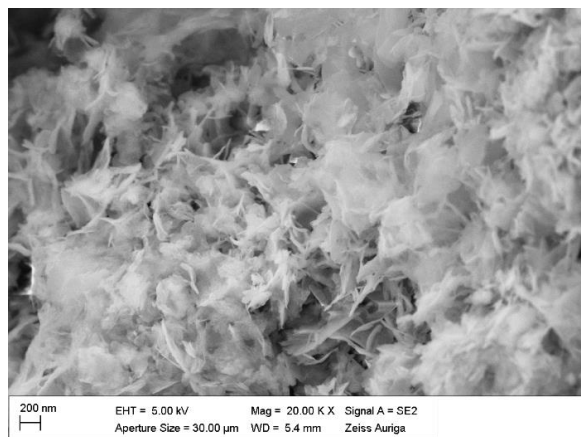


Figure 5. SEM images of ZnGa LDH and Ga/ZnGa samples calcined at different temperatures.

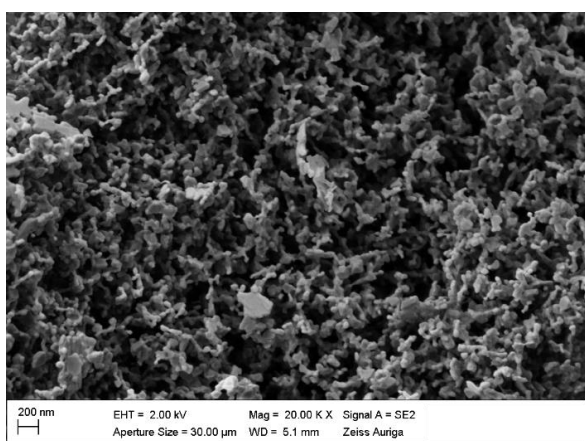
ZnAl (50 k)



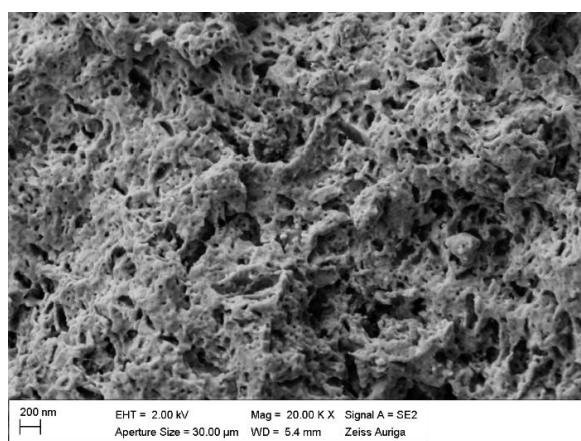
Ga/ZnAl



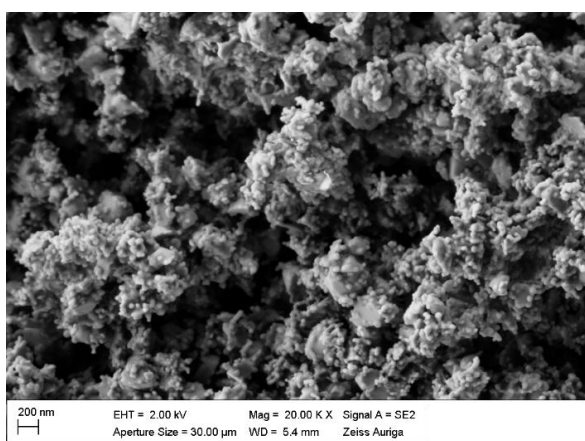
ZnAl\_750



Ga/ZnAl\_750



ZnAl\_925



Ga/ZnAl\_925

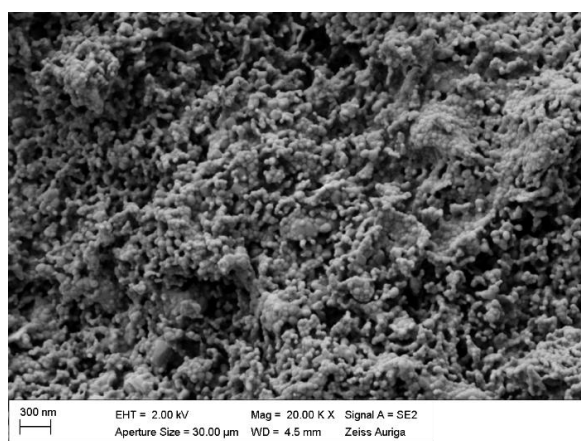


**Figure 6.** SEM images of ZnAl and Ga/ZnAl samples calcined at different temperatures.

Results revealed that the morphology of the samples was strongly influenced by both the composition of the initial LDHs and the temperature of the calcination temperature. ZnGa appears as smooth and

relatively uniform platelets, with about 15-18 nm thickness and quite irregular shape, but relatively uniform sizes, without sharp corners. During the calcination procedure, the morphology changes gradually. Small almost spherical balls begin to form at 750°C, coexisting with the initial sheets, still in majority. Finally, at 925°C, bulk polyhedra closely packed with each other are formed.

After the calcination of ZnGa at a temperature of 750°C, the transitions towards the ZnGa<sub>2</sub>O<sub>4</sub> and Ga<sub>2</sub>O<sub>3</sub> brings also spectacular morphology transformations. A high number of small, uniform holes appear on the sheets surface at 750°C, while the sheets become less plane and wider. At 925°C, the transition to final phases also leads to numerous polyhedra, quite well individualized and characterized by a high dimensional dispersity (size between 50-300 nm). ZnAl looks typically as a LDH, consisting of platelets nanoparticles with sizes around 150 nm, interconnected to each other. Upon heating, the morphology changes to numerous grains, almost spherical, loosely grouped to each other at 750°C, and transformed in bulk, porous agglomerations at 925°C. The reconstruction product looks very alike the native ZnAl, with the smooth thin sheets arranged under different angles, typically for a LDH. The reconstruction success is also confirmed by the SEM results. Upon calcination at 750°C, a sponge-like mass is formed from small spherical grains tightly packed. A very similar morphology is noticed after calcination at 925°C, based on particles with a higher diameter; these results are in accordance with the XRD patterns that were highly similar for these two samples (figure 2). TEM data reveal the morphology changes during the calcination from 600 to 750°C. The particles are closely packed after calcination at 600°C with relatively uniform sizes of 15-20 nm. Upon calcination at 750°C, the particles diameter increase up to 30-50 nm, pointing out the formation of well-individualized, relatively uniform and close packed particles for the Ga/ZnAl 750 sample (figure 7).

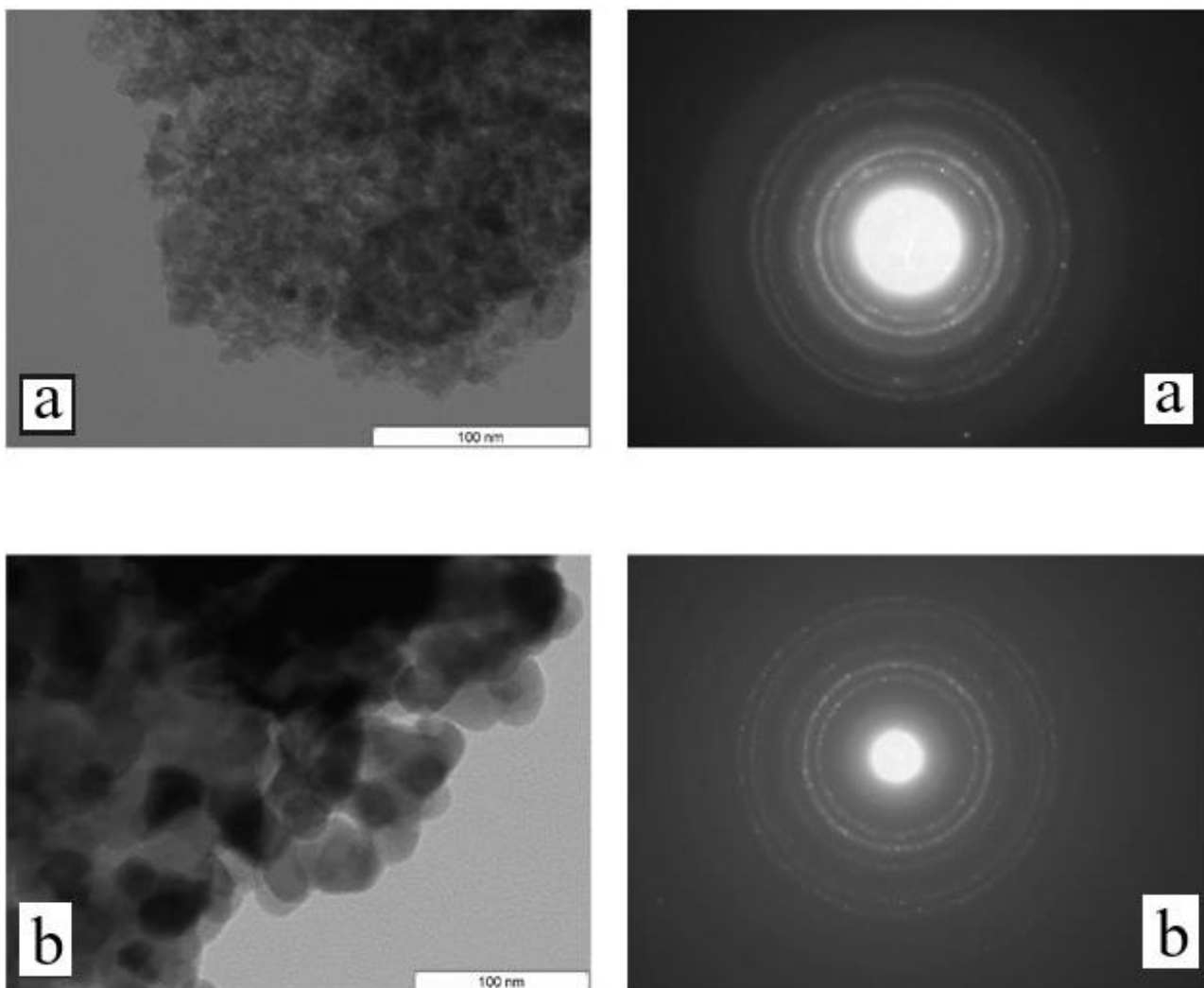


**Figure 7.** TEM images and SAED of Ga/ZnAl<sub>600</sub> (a) and Ga/ZnAl<sub>750</sub> (b) samples; light field (left) and dark field (right).

The BET specific surface areas (SSA) values are presented in Table 4. The samples containing aluminum have higher SSA by comparison with the samples based on gallium. It is interesting to note that the SSA values of the initial LDHs are lower than those of the reconstructed materials, both for aluminum and gallium-based samples. Also, the calcination process at 750°C let to the increasing of the surface area. This behavior is consistent with similar results from the literature [23, 24].

**Table 4:** Specific surfaces of the samples

Sample	SSA, m <sup>2</sup>	Sample	SSA, m <sup>2</sup>
ZnAl	74	ZnGa	69
Ga/ZnAl	83	Ga/ZnGa	75
Ga/ZnAl_750	91	Ga/ZnGa_750	89

The XRF analysis was used to determine the samples elemental composition in the nearby of the surface (Table 5). In the as-synthesized samples, the 3:1 ratios between the divalent/trivalent ions from the synthesis recipe are roughly found also in the solids. During the reconstruction step, the surface of the ZnGa strongly enriches in gallium. A high amount of sulfate ions, detected as sulfur on the surface, indicate the deposition of some gallium sulfate nanoparticles on the surface during the regeneration of the structure. For Ga/ZnAl calcined at high temperature, aluminum is found in a higher concentration than expected, while zinc content was unexpectedly low that shows a strong diffusion of aluminum from the bulk material to the surface of the grains.

**Table 5:** Elemental composition of samples determined by XRF analysis

Sample	Element	Conc (%)
ZnAl	Zn	75
	Al	25
ZnGa	Zn	73.7
	Ga	26.3
Ga/ZnGa	S	27
	Zn	5
	Ga	68

Ga/ZnAl_925	Al	43
	S	0.1
	Zn	32
	Ga	25

Further, the EDX was also used to study the samples composition. The results are shown in Figure 8.

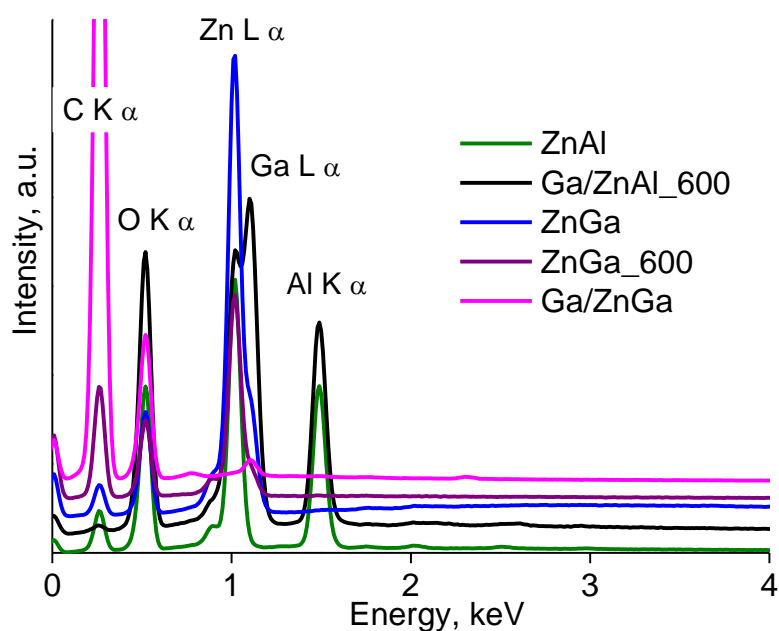


**Figure 8.** EDX spectra of the samples

The reconstructed Ga/ZnGa has a higher content in C and O by comparison to the assembly of oxides revealing the presence of  $\text{CO}_3^{2-}$  anions.

Further, XPS analysis was used to get information about the surface composition of the materials (see Figure 9 and Table 6).

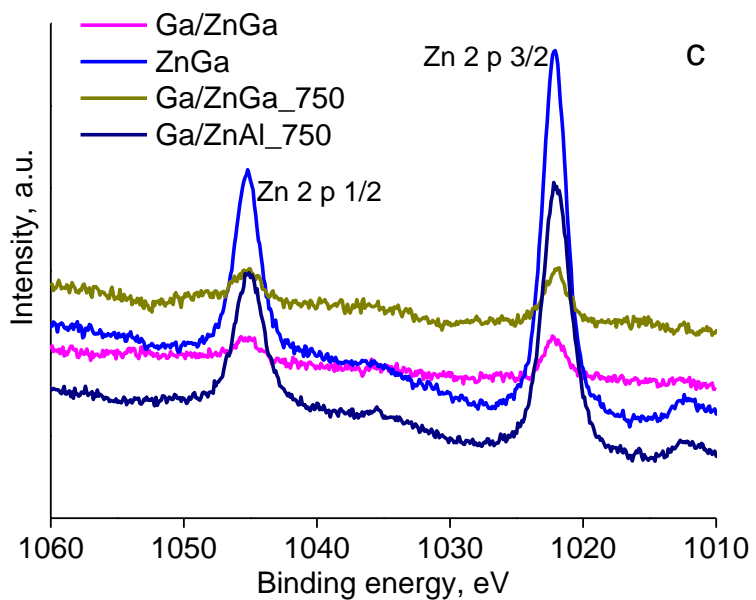
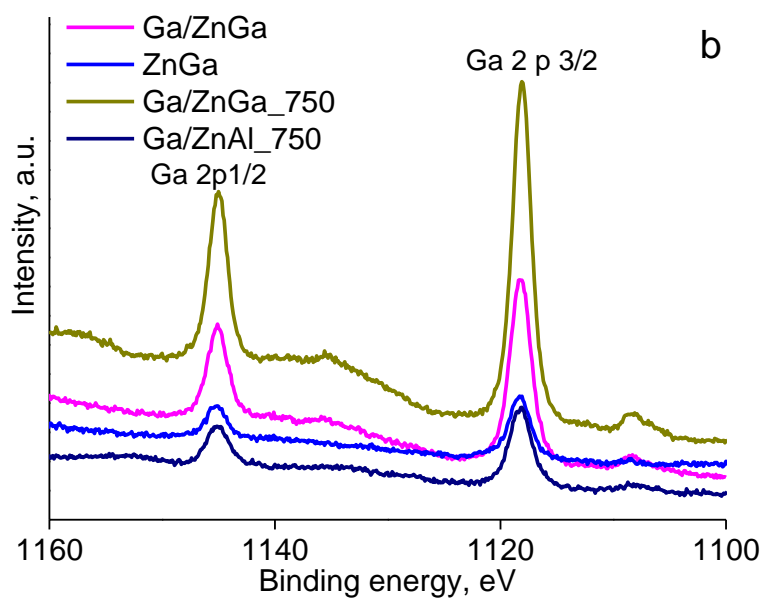
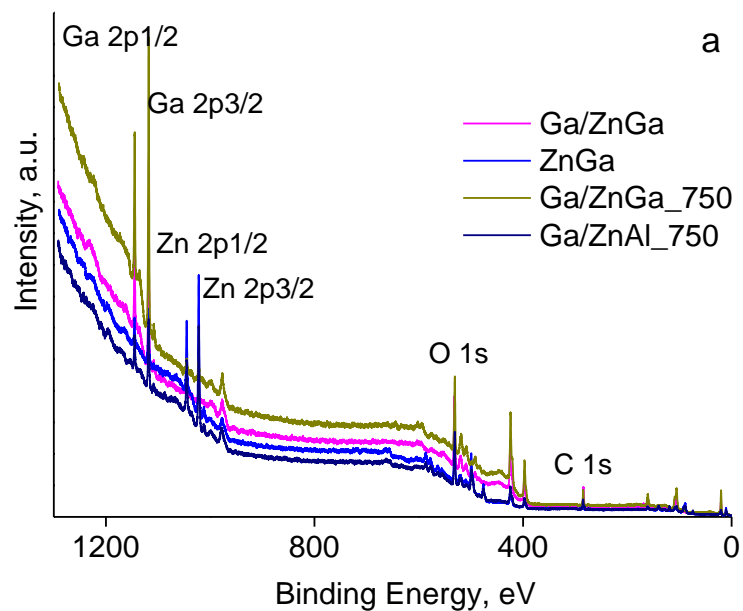


**Figure 9.** XPS spectra of the samples a. overall spectra; b. Ga<sub>2</sub>p<sub>1/2</sub> and Ga<sub>2</sub>p<sub>3/2</sub>; c. Zn<sub>2</sub>p<sub>3/2</sub>.

The main signals from the XPS spectra are due to gallium oxide 1118-1120 eV (Ga 2p<sub>3/2</sub>), 1145 eV (Ga 2p<sub>1/2</sub>), zinc oxide 1045 (2p<sub>1/2</sub>) and 1022 eV(2p<sub>3/2</sub>) and aluminum oxide, 80 eV (2p) [22, 25, 26]. The oxygen signal O1s from oxides appears between 530.8-531.9 eV. The peaks are symmetric and well-centered, indicating that the metals are present only in the oxides forms.

**Table 6:** Chemical composition of the samples determined by XPS.

	Ga/ZnAl_600	Ga/ZnAl_750	ZnGa	ZnGa_600	Ga/ZnGa	Ga/ZnGa_750
O/Metal	2.24	1.91	2.19	0.77	0.85	1.80
Zn/Ga	2.43	1.89	3.42	7.74	0.14	0.11
Zn/Al	2.76	1.72	-	-	-	
Al/Ga	0.88	1.10	-	-	-	

The results shown in Table 6 indicate that the composition of the samples strongly depends on the thermal treatment. For ZnAl, after reconstruction in Ga<sub>2</sub>(SO<sub>4</sub>)<sub>3</sub> solution followed by calcination at 600°C, the gallium amount increased such that gallium content reaches a ratio of about 88% regarded to aluminum content. The content of ZnAl<sub>2</sub>O<sub>4</sub> and ZnGa<sub>2</sub>O<sub>4</sub> is almost equal for both assemblies of the mixed oxides. Upon calcination at 750°C, the Al/Ga ratio increases, suggesting the advanced diffusion of gallium in the inner grains during the high temperature treatment. Both Zn/Al and Zn/Ga ratios are 1.72 and 1.89, respectively, indicating that ZnO is present as a separate phase, in order to balance the expected 1/2 molar ratio from ZnAl<sub>2</sub>O<sub>4</sub> and ZnGa<sub>2</sub>O<sub>4</sub> phases. For ZnGa LDH Zn/Ga ratio is higher than 3 suggesting that some gallium does not precipitate during the synthesis. The calcination at 600°C dramatically increases the Zn/Ga ratio, suggesting a migration of gallium in the inner part of the grains. The reconstruction of the structure brings an amazing enrichment of the particles in gallium, suggesting that its presence as octahedra in the layer is doubled by the formation

of a high amount of nanoparticles, undetectable by XRD, on the outer surface of the LDH grains. The formation of high amounts of Ga<sub>2</sub>O<sub>3</sub> that is revealed by XRD, is also reflected in the final Zn/Ga ratio of 0.11. There are significant differences in the behavior of the two series of samples, due to the presence of aluminum together with gallium in the ZnAl series. Aluminum hinders the strong segregation of gallium oxide phase, which is very abundant in ZnGa-derived materials.

### 3. Conclusions

Nanoscaled assemblies of Zn-Al-Ga mixed oxides were obtained by the controlled thermal treatment of Zn<sup>2+</sup>Me<sup>3+</sup> (Me = Al/Ga) layered double hydroxides (LDHs) precursors, as their “as-synthesized” form or reconstructed in the aqueous solution of Ga<sub>2</sub>(SO<sub>4</sub>)<sub>3</sub>. The derived ensembles of the mixed oxides are clearly identified as ZnO/ZnAl<sub>2</sub>O<sub>4</sub>/ZnGa<sub>2</sub>O<sub>4</sub> and ZnO/Ga<sub>2</sub>O<sub>3</sub>/ZnGa<sub>2</sub>O<sub>4</sub>, while their nano-sized features, described as nanoparticle sizes and their interspaces, are impacted by the composition of the LDH precursors and the calcination temperature used during the transformation of the 2D-layered structure of the LDH into the mixed oxides. These results demonstrate that the synergistic combination of various methodologies in production of the assemblies of the mixed oxides from LDHs might afford to tune their nanoarchitectonic into an effective tool for designing innovative materials.

### Acknowledgements

The authors are grateful for the financial support from the Romanian National Authority for Scientific Research and Romanian Ministry of Research, project number PN-III-P2-2.1-PED-2016-0473, acronym ELECTROPHOTO.

### References

1. Vaccari, A. *Catalysis Today* **1998**, *41*( 1–3), 53-71.
2. Mishraa, G.; Dasha, B.; Pandey, S. *Applied Clay Science* **2018**, *153*, 172–186.

3. Marcu, I. C.; Urdă, A.; Popescu, I.; Hulea, V. Layered Double Hydroxides-Based Materials as Oxidation Catalysts. In *Sustainable Nanosystems Development, Properties, and Applications*; Putz, M. V.; Mirica, M. C.; Ed.; IGI Global, 2017; pp. 59-121.
4. Bukhtiyarova, M. V. *J. Solid State Chem.* **2019**, *269*, 494–506.
5. Prince, J.; Tzompantzi, F.; Mendoza-Damián, G.; Hernández-Beltrán, F.; Valente, J. S. *Appl. Catal. B: Environ.* **2015**, *163*, 352–360.
6. Tanasoi, S.; Mitran, G.; Tanchoux, N.; Cacciaguerra, T.; Fajula, F.; Sandulescu, I.; Tichit, D.; Marcu, I. C. *Appl. Catal. A: Gen.* **2011**, *395*, 78–86.
7. Mitran, G.; Cacciaguerra, T.; Loridant, S.; Tichit, D.; Marcu, I. C. *Appl. Catal. A: Gen.* **2012**, *417–418*, 153–162.
8. Mascolo, G.; Mascolo, M. C. *Microp. Mesop. Mater.* **2015**, *214*, 246-248.
9. Puscasu, C. M.; Carja G.; Mureseanu, M.; Zaharia, C. *IOP Conf. Ser.: Mater. Sci. Eng.* **2017**, *227*, 012105, 8 pages, doi:10.1088/1757-899X/227/1/012105.
10. Kawamura, S.; Ahmed, N.; Carja, G.; Izumi, Y. *Oil Gas Sci. Technol.* **2015**, *70(5)*, art. number A841, 841-852.
11. Carja, G.; Birsanu, M.; Okada, K.; Garcia, H. *J. Mater. Chem. A* **2013**, *1(32)*, 9092-9098.
12. Carja, G.; Kameshima, Y.; Ciobanu, G.; Okada, K. *J. Nanosci. Nanotechnol.* **2010**, *10 (4)*, 2880-2884.
13. Hernández-Hernández, L. A.; Aguilar-Hernández J. R.; Moure-Flores, F. de; Melo-Pereirac, O. de; Mejía-García, C.; Cruz-Gandarilla, F.; Contreras-Puente, G. *Mater. Res.* **2017**, *20(6)*, 1707-1712.
14. L. Zou, L.; Xiang, X.; Wei, M.; Li, F.; Evans, D. G. *Inorg. Chem.* **2008**, *47*, 1361.
15. Marie, P.; Portier, X.; Cardin, J. *Phys. Stat. Sol. A: Appl. Mater. Sci.* **2008**, *205 (8)*, 1943-1946.
16. Quan, Y.; Fang, D.; Zhang, X.; Liu, S.; Huang, K. *Mater. Chem. Phys.* **2010**, *121*, 142–146.
17. Kumar, S.; Sarau, G.; Tessarek, C.; Bashouti, M. Y.; Hähnel, A.; Christiansen, S.; Singh, R. *J. Phys. D: Appl. Phys.* **2014**, *47*, 435101-435111.

18. Patil, P.; Parka, J.; Lee, S. Y.; Parka, J. K.; Cho, S-H. *Appl. Sci. Conver. Technol.* **2014**, *23(5)*, 277-281.
19. Zhuang, Y.; Ueda, J.; Tanabe, S. *Opt. Mater. Expr.* **2012**, *2(10)*, 1378-1383.
20. Daniele, S.; Tchekoukov, D.; Hubert Pfalzgraf, L.G. *J. Mater. Chem.* **2002**, *12*, 2519–2524.
21. Zak, A. K.; Razali, R.; Abd Majid, W.H.; Darroudi, M. *Int. J. Nanomed.* **2011**, *6*, 1399–1403.
22. Carja, G.; Grosu, E. F.; Mureseanu, M; Lutic, D. *Catal. Sci. Technol.* **2017**, *7*, 5402-5412.
23. Kim, K.; Gwak, G.-H.; Okada, T.; Oh, J.-M.; *J. Solid State Chem.* **2018**, accepted manuscript, <https://doi.org/10.1016/j.jssc.2018.03.041>.
24. Starukh, H.; Levytska, S. *Appl. Clay Sci.* **2019**, *180*, 105183 (6 pages).
25. <http://www.xpsfitting.com/2008/09/zinc.html> (accessed June 24<sup>th</sup>, 2019).
26. <https://xpssimplified.com/elements/gallium.php> (accessed June 24<sup>th</sup>, 2019).